Novel two-dimensional photonic crystals designed by evolutionary algorithms

Stefan F. Preble*[a], Hod Lipson[b], Michal Lipson[a]
[a]School of Electrical and Computer Engineering;
[b]Schools of Mechanical & Aerospace Engineering and Computing & Information Science,
Cornell University, Ithaca, NY 14853, USA

ABSTRACT

We use evolutionary algorithms to search the space of two-dimensional photonic crystals with maximum bandgaps for a given index contrast. The unit-cells of the photonic crystal are represented as bitmaps which are either directly encoded or generated through bottom-up and top-down construction trees. The fitness criterion rewards for partial band gaps and is evaluated by solving for the photonic crystals bands using an eigensolver in a planewave basis. Starting from random patterns and with no prior knowledge, the process discovered a number of novel photonic crystals, some with bandgaps that are 12.5% larger than any previously reported human-designed crystals.

Keywords: Photonic Crystals, Evolutionary Algorithm, Design Automation

1. INTRODUCTION

The first photonic crystals were not designed and fabricated in a laboratory but were evolved over millions of years in nature. They create the beautiful colors in butterfly wings[1] and are even found in creatures of the sea such as the Sea Mouse[2]. Photonic crystals possess a photonic bandgap[3-5] – a range of frequencies where light is forbidden from propagating in the crystal. By creating defects[6] in the photonic crystal, light with a frequency in the bandgap can be guided or trapped, enabling the control of the flow of light on the nanoscale[4]. Photonic crystals were traditionally designed by trial and error with some insight from the extensive research of crystalline atomic lattice structures[4,7]. This has yielded simple lattices and unit cells, such as a square lattice of cylinders[5]. The large bandgap of these photonic crystals has been achieved by varying the parameters of the lattice, however, it is not known whether these simple structures truly achieve the maximum permissible bandgap for a given index contrast.

In this work we use an evolutionary algorithm to search for novel photonic crystals with maximal bandgaps. Evolutionary algorithms[8,9,10] are inspired by natural evolution, and operate by repeatedly varying, selecting, and replicating successful individuals in a population of candidate solutions. Evolutionary algorithms are very well suited for finding solutions to problems that involve very large and complex search spaces that do not have smooth gradients leading to an optimum, but have some other useful substructure. In particular, evolutionary algorithms are well suited for searching open-ended design spaces that are not conveniently characterized by a finite set of parameters, such as the space of functional geometries and morphologies[11,19]. Evolutionary algorithms have been shown to be effective tools for exploring hard design challenges, and have recently proven to be an effective design automation tool that can sometimes outperforms human design[10].

The evolutionary algorithm used here starts with a population of randomly generated photonic crystals that in general possess no bandgap. The fittest photonic crystals, those approaching higher band gaps, are selected and mated with each other. During mating the elements of the parent photonic crystals are crossed over (swapped), and are then subject to mutation (randomly changing high/low dielectric constants). This process is repeated for many generations after which we find photonic crystals that not only have bandgaps, but also have bandgaps larger than the ones created by humans.

Previous works have seeded the evolutionary algorithm with a human made photonic crystal with a known bandgap, in turn, only optimizing the bandgap of seed crystal[12]. In this work, we are able to achieve large bandgaps without seeding, opening the possibility for the algorithm to find photonic crystals that would have never otherwise been imagined by

humans. In contrast to previous works[12] that focus on higher energy bands we only focus on a bandgap between the first two bands because the lower energy bandgap should fall under the light-line, enabling practical fabrication in a thin dielectric slab system[4].

2. METHODOLOGY

In this paper the unit cell is the element of the photonic crystal that is subject to evolution. The unit cells are discretized onto a 32x32 grid of square pixels consisting of high (3.4 - Silicon) or low (1 - Air) dielectric material. To apply the evolutionary algorithm to the design of the photonic crystal, the unit cell is represented by a chromosome – a blueprint of the makeup of the cell. We look at two types of chromosome representations in this paper: bitmaps (direct encodings) and trees (generative encoding). Both bottom-up and top-down trees are explored.

The bitmap representation consists of a binary string of length 1024 (32×32) where a '1' corresponds to high dielectric material, and a '0' corresponds to a low dielectric material. Each bit in the binary string corresponds to a unique grid point of the 32x32 unit cell, as shown in Figure 1. In this representation there are 2^{1024} possible photonic crystals.

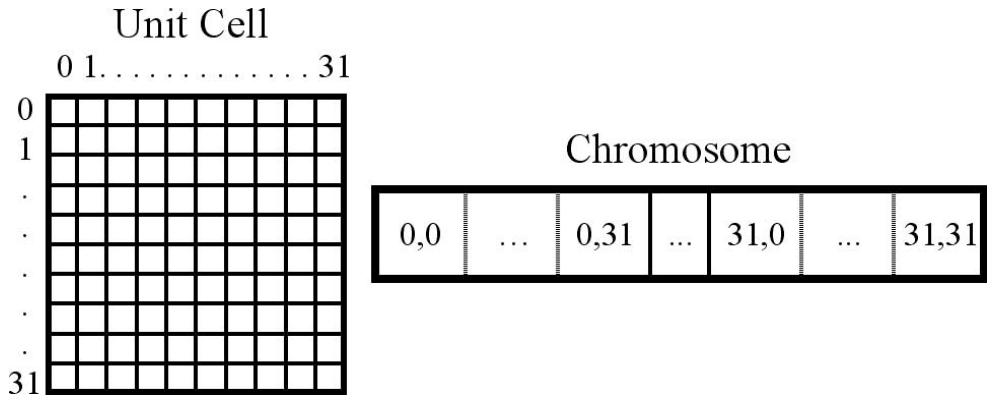


Fig. 1. A unit cell discretized onto a 32x32 grid and its associated binary string. The binary string encodes the unit cell row –by- row. Each pixel in the unit cell is assigned to be high or low dielectric material.

The tree representations define the unit cell using 'clumps' of high or low dielectric material. This is a much more efficient representation, since photonic crystals generally have clumps of dielectric material, as opposed to isolated pixels. This efficiency allows the evolutionary process to better exploit the substructure of the search space. In the top down tree representation the unit cell is recursively split into subdivisions by partition lines, starting at the top of the tree and going down. At the bottom of the tree are terminal nodes that determine the dielectric material (0 or 1) of the corresponding subdivision. The lines that split the unit cell are uniquely identified by their start and end points, where the start and end points lay on the outside perimeter of the unit cell. Tree nodes to the right of a split are inclusive, so that all pixels that have a position 'greater than or equal' to the split-line are included. Tree nodes to the left of a split are exclusive, so that all pixels that have a position 'less than' the split-line are included. An illustration of this representation and how it is interpreted into the pixilated unit cell is shown in Figure 2a.

In the bottom-up tree representation rectangles of dielectric material are recursively combined to form a larger structure. The rectangles are defined by a width and height, center, and a dielectric material (0 or 1). Going up the tree, the rectangles are combined by the Boolean operators AND and OR. An illustration of this representation and how it is interpreted into the pixilated unit cell is shown in Figure 2b.

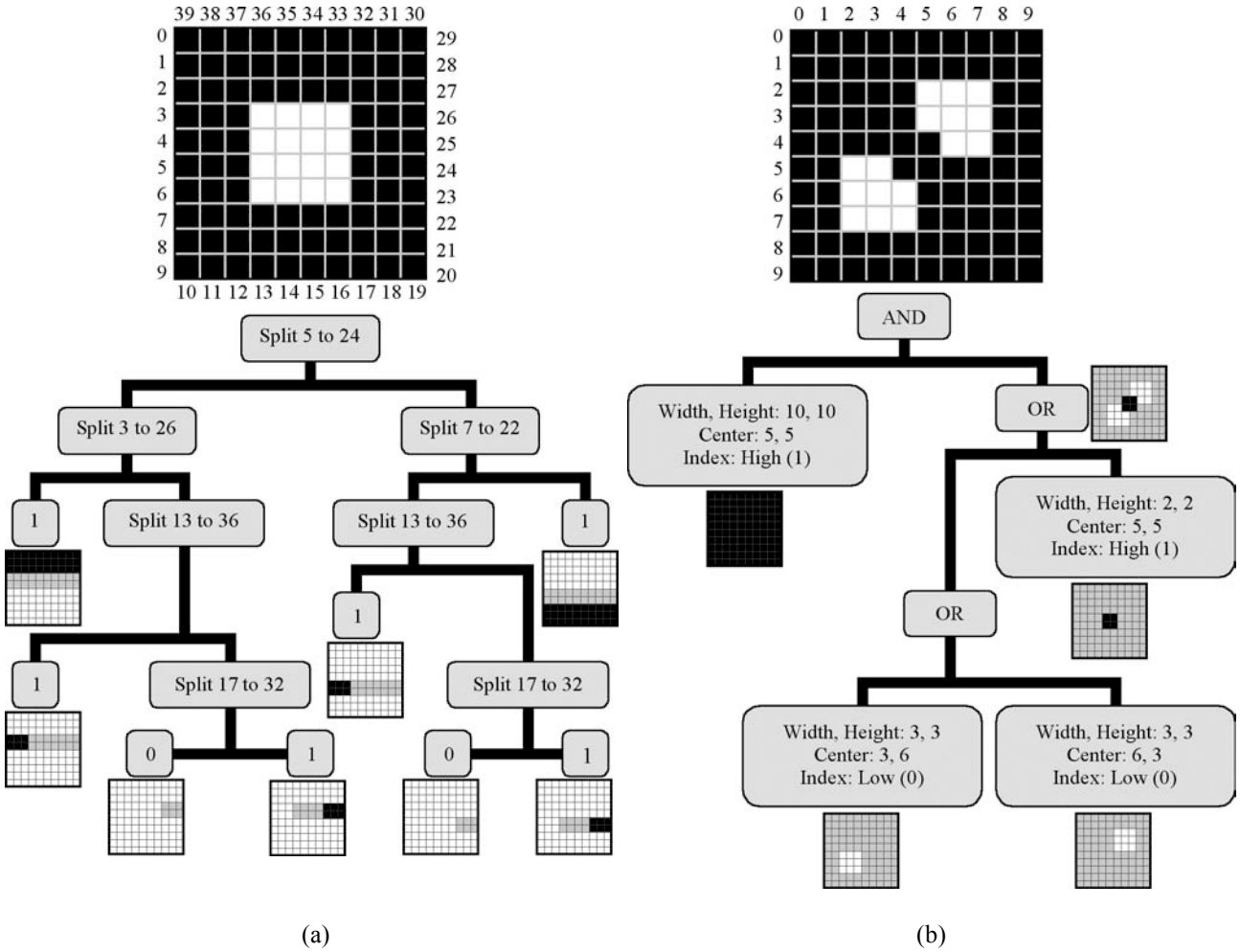


Fig. 2. (a) Illustration of an example 10x10 unit cell (32x32 is used with the evolutionary algorithm) and a top-down tree that can be used to construct this unit cell. The black (white) pixels are high (low) index material. The numbers label the perimeter of the unit cell. Starting at the top of the tree and going down, each split, a dividing line uniquely defined by two perimeter pixels, sections the unit cell into ever-smaller areas. The terminal nodes assign dielectric material (i.e. high or low) to these areas. Next to each terminal node is an illustration of the result. Light-gray coloring designates the sub-area that has been defined by the splits (i.e. the terminal nodes sibling 'acts' on this light-gray area). The complete unit cell is obtained by combining all of the sub-areas into one. (b) Illustration of an example 10x10 unit cell (32x32 is used with the evolutionary algorithm) and a bottom-up tree that can be used to construct this unit cell. The numbers around the unit-cell label the x-y grid. Starting at the bottom of the tree and going up, rectangles defined by a width, height, center and index are combined using boolean AND and OR operator nodes. The illustrations next to the nodes show how the rectangles are defined and combined to obtain the unit cell. The light-gray coloring indicates that those pixels are undefined and the boolean operators subsequently have no effect on them (i.e. defaults to OR). If there are any undefined pixels in the resulting unit cell, they are automatically set to be low index material.

The evolutionary algorithm used here operates in the following steps:

Step 1: Initialization. The evolutionary algorithm starts with a population of 100 randomly generated chromosomes. In the bitmap representation each pixel in the unit cell has a 50% probability of being high or low index material. In the top town tree representation, the top node is a randomly generated split. The children nodes are randomly generated to be a split, or a high or low index terminal node, all with equal probability. In the bottom up representation, the top node is a randomly generated boolean operator. The children nodes are randomly generated to be one of the boolean operators, or a rectangle of dielectric material, with equal probabilities.

Step 2 – Fitness evaluation: Each chromosome in the population is then converted into a 32x32 unit cell. The high (low) index pixels are assigned an index of 3.4 (1). The unit cell is then repeated on a square lattice of period *a*. Next, the bands of the photonic crystal are calculated and any bandgap (or lack of) is obtained. A software package was used to solve for the bands of the photonic crystal by preconditioned conjugate-gradient minimization of the block Rayleigh quotient in a planewave basis[13].

In previous works[12] the fitness criteria used was the gap to mid-gap ratio:

$$\text{Fitness} = \frac{E_{top} - E_{bottom}}{E_{middle}} \qquad \text{Eq. 1}$$

where E_{top}, E_{bottom}, E_{middle} are the top, botton and the middle of bandgap, respectively. However, since the initial population of randomly generated photonic crystals in general *does not* possess a bandgap, they were artificially assigned a small fitness value[12]. A search using such a fitness criterion has no gradient to follow during the initial phase, and therefore drifts blindly in the search space. The lack of gradient may explain why previous attempt that used this fitness criterion eventually needed to seed the population with a hand-designed solution with an existing bandgap. In this work we have developed a fitness criterion that is suitable for crystals that do not already possess a bandgap, thereby enabling the discovery of new types of photonic crystal structures from scratch. Our measure of fitness is the amount of overlap of the top and bottom bands, here referred to as the overlap area. Since no assumptions were made about the symmetry of the unit cell it is necessary to calculate the bands over the entire first brillouin zone. Figure 3 shows a band diagram for a randomly generated photonic crystal that does not possess a bandgap. Only the first brillouin zone points along the Γ→X1→M→X2→Γ quadrant are shown for compactness. It is clear that there is no bandgap between the bands but there is a significant overlap.

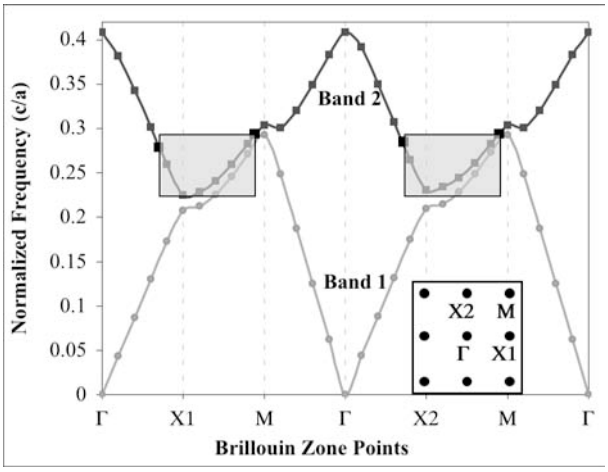


Fig. 3. Band diagram of a randomly generated photonic crystal with no bandgap. The vertical axis is the frequencies normalized to (c/a) where 'c' is the speed of light and 'a' is the lattice period. The horizontal axis are the brillouin zone points. The inset shows the reciprocal lattice and the corresponding Brillouin zone points. The shaded light-gray boxes indicate the areas where the two bands overlap each other. The bounds of the boxes are obtained from the points in the band diagram where the top band is below the top of band 1. The height of the boxes is always the same; it's defined from the bottom of band 2 (At the X1 point) to the top of band 1 (At the M point). The width is from the left-most to the right-most points (including the interpolated 'half-way' points) that fall below the top of band 1. The total overlap area (Eq. 2) can be obtained from the sum of the areas of the individual shaded boxes.

The amount of overlap is defined by an overlap area:

$$\text{Overlap Area} = \frac{E_{top,1} - E_{bottom,2}}{\left(E_{top,1} + E_{bottom,2}\right)/2} \cdot \frac{N_{overlap}}{N_{total}} \qquad \text{Eq. 2}$$

where $E_{top,1}$ is the top of the bottom band, $E_{bottom,2}$ is the bottom of the top band, $N_{overlap}$ is the number points in the band diagram where the top band is below the top of the bottom band, and N_{total} is the total number of points (i.e. the individual dots in Figure 3). To improve the speed of the band calculations, only four points between each Brillouin zone symmetry point (i.e. Γ, X1, M, X2) was calculated, so an additional point is linearly interpolated 'half-way' between each one of the points. This interpolation is shown in Figure 3 where the left and right edges of the two overlap areas don't fall on points that were actually calculated, they fall on the 'half-way' points, as indicated by the bold square points (these are the only half-way points shown on this diagram). For photonic crystals that do posses a bandgap, the traditional fitness criteria (Eq. 1) is used.

Step 3: Selection. – The 100 chromosomes are then selected for the next generation using a fitness-dependent selection criterion. Two selection methods were used: The first is rank selection, where the likelihood of an individual being selected is proportionate to its rank in the population (i.e. the photonic crystals are ranked from largest to smallest overlap to smallest to largest bandgap). A stochastic-uniform-sampling (SUS) method was used to implement the selection in a way that guarantees minimal selection noise[9]. The second selection method used was deterministic crowding[14] (DC), which helps maintain diversity of solutions by comparing solutions only to those that are most similar to them. Diversity of solutions in the population must be maintained if crossover-operators are expected to produce anything new. Selected chromosomes become the parents for a new generation of chromosomes.

Step 4: Variation: – Two new offspring are created from two selected parents. To create the children chromosomes, portions of the two parent chromosomes are crossed over with a crossover probability of 70% (i.e. 30% of the time the children are exact copies of the parents). In the bitmap representation, two random points in the 32x32 unit cell are picked. All of the pixels in the rectangle defined by these two points are swapped between the parents to create the new children. The order of the two points (i.e. point 1 or 2) determines how the rectangle is defined. If point 2 is farther away from the origin (i.e. greater) than point 1, then the rectangle spans from point 1 (upper-left corner of rectangle) to point 2 (lower-right corner of rectangle). If point 2 is closer to the origin than point 1, then the rectangle spans from point 1 in one unit-cell to the neighboring unit-cells. However, since the chromosome only encodes the one unit-cell and not a periodic array of them, the rectangle must be wrapped back into the one unit-cell (i.e. where point 1 is). This is done by moving the portions of the rectangle in the neighboring-cells to their equivalent positions in the 'main' unit-cell, as illustrated in Figure 4. In the tree representations, a random node in each of the two parent trees is selected. Then the nodes and all of their respective children are swapped between the two parents trees to obtain the two new children.

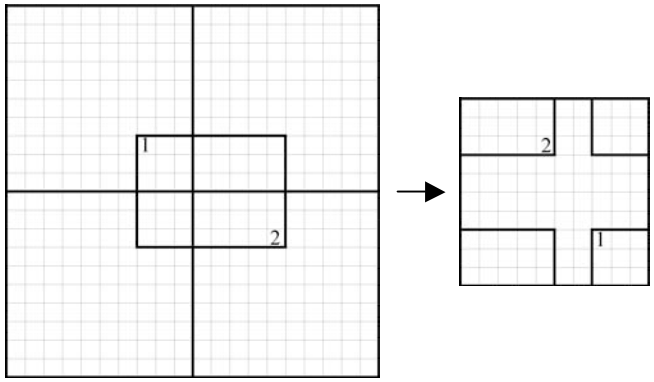


Fig. 4. An example rectangle that spans from point 1 in the 'main' unit-cell to points in the neighboring unit-cells. This representation is equivalent to a rectangle that spans the corners of the 'main' unit-cell.

In the next step of variation the chromosomes in the new population are mutated. In the bitmap representation, each bit in the 1024 bit long chromosome is subject to be flipped from a 0 to a 1 or vice versa with a mutation probability of 1%. In the tree representations, each node in the tree is mutated with a probability of 1%. The manifestation of the mutation depends on the type of node. For a split node, the start and end points are randomly offset by ± 1 or 0, each with an equal probability. A terminal node can switch from high to low dielectric material or vice-versa. A Boolean operator node can switch from AND to OR or vice-versa. And lastly, for a rectangle node, the width, height, and center can each be offset by ± 1 or 0, with equal probability.

In open-ended tree representations, variation is followed by pruning. To keep the tree from becoming overly large, which is very likely to happen from crossover, the trees are pruned to be a maximum number of levels in order to control the depth of the trees (the breadth is automatically controlled by this). Unfortunately the pruning has the unwanted effect that it may blindly destroy a tree that would otherwise have a very high fitness. To minimize this risk the number of levels that the trees are pruned to was tuned over many trials to minimize the effect. The next step also helps to minimize the risk.

Step 6: Elitism: It is important to ensure that the fitness of the population does not decrease in this newly created population. This is done by practicing elitism – a random chromosome in the new population is replaced with the best chromosome from the previous generation.

Step 7– Repeat from step 2 until a stopping criterion is met.

3. RESULTS AND DISCUSSION

The evolutionary algorithm was run for 1500 generations to obtain large bandgaps for the TE Polarization (electric field in the plane of the photonic crystal) of light. The evolutionary algorithm could easily be applied to the TM polarization, as well. First we consider the evolutionary algorithm using the stochastic-uniform-sampling selection criterion (SUS). After the 1500 generations, using the bottom-up tree and top-down tree representations, the SUS evolutionary algorithm yielded photonic crystals with bandgaps as large as 30.86% and 31.89%, respectively, as shown in Figure 5. The band diagram for the top-down tree photonic crystal is shown in Figure 6. However, the bitmap representation achieved a bandgap of only 5.12%. This was improved upon by using a coarser grid of 16x16 pixels, as shown in Figure 7.

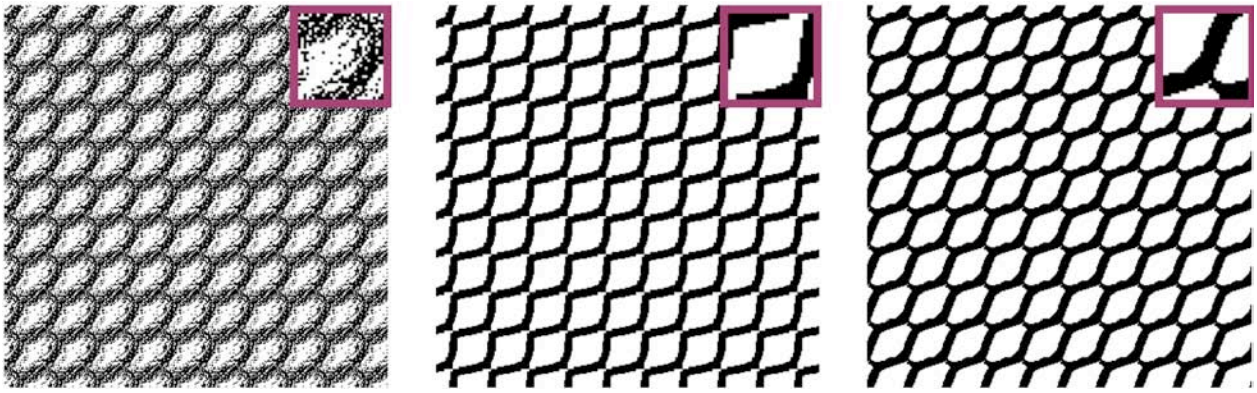


Fig. 5. Photonic crystals and unit-cells (insets) created by the SUS evolutionary algorithm. From left to right: Bitmap Representation (5.12% Bandgap), Bottom up tree (30.86% Bandgap), Top down tree (31.89% Bandgap)

It is clear from these results that the tree representations considerably outperformed the bitmap representation. This is because the trees are able to encode the information in the unit-cell much more efficiently than a bitmap. The bitmap representation yields a lot of extra 'noise', or random pixels that degrade the quality of the photonic crystal, as seen in Figure 7 and especially in Figure 5 where the search space is extremely large (2^{1024} possible solutions). The random pixels effectively reduce the index-contrast, so by manually removing the noise the bandgap can be improved considerably (even for the 32x32 grid where there clearly is a photonic crystal that is capable of supporting a bandgap,

there is just too much noise), but doing so is time-consuming and undesirable for general design purposes. The tree representations are much less susceptible to this noise problem since they deal hierarchically with 'clumps' of dielectric material as opposed to individual pixels.

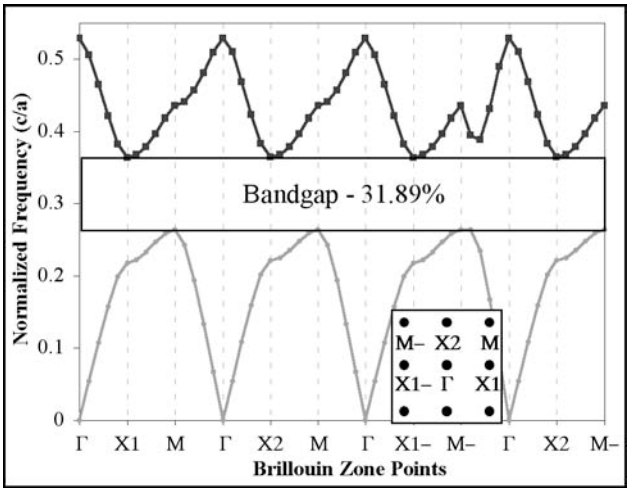


Fig. 6. Band diagram of the photonic crystal discovered by the SUS evolutionary algorithm using a top down tree representation. The vertical axis is the frequencies normalized to (c/a) where 'c' is the speed of light and 'a' is the lattice period. The horizontal axis is the brillouin zone points. The inset shows the reciprocal lattice and the corresponding Brillouin zone points.

Figure 8 shows some performance metrics of the SUS evolutionary algorithm, plotted as function of generation. Figure 8a shows the best fitness for the different representation types. For fitness values below 1 the fitness is the overlap area, for values above 1 the fitness is the bandgap, i.e. a fitness of 1.25 is a bandgap of 25%. Figure 8b shows the average hamming distance of the population. The hamming distance is a measure of how different the photonic crystals in the population are. The larger the hamming distance, the more diverse the population. It is important to maintain a diverse population as long as possible because otherwise the growth of the over-all population is stunted since all of the photonic crystals become essentially the same. Once the crystals are very similar, crossover between parents becomes rather ineffective. Consequently, the algorithm may prematurely converge to only a local maximum, rather than a global maximum. It is clear from Figure 8 that the evolutionary algorithm converges to a solution rather quickly, within only 100 generations. This is a weakness of the stochastic-uniform-sampling evolutionary algorithm. We now consider another type of selection criterion, deterministic crowding, that is slower to converge but is able to maintain a very diverse population, thereby delaying convergence and promoting useful crossover.

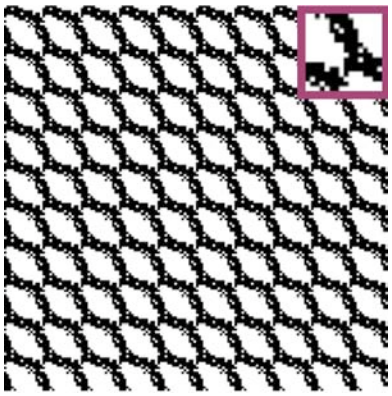


Fig. 7. Photonic crystal and the unit-cell (indent) obtained using the bitmap representation with a 16x16 grid. The bandgap of the photonic crystal is 21.92%.

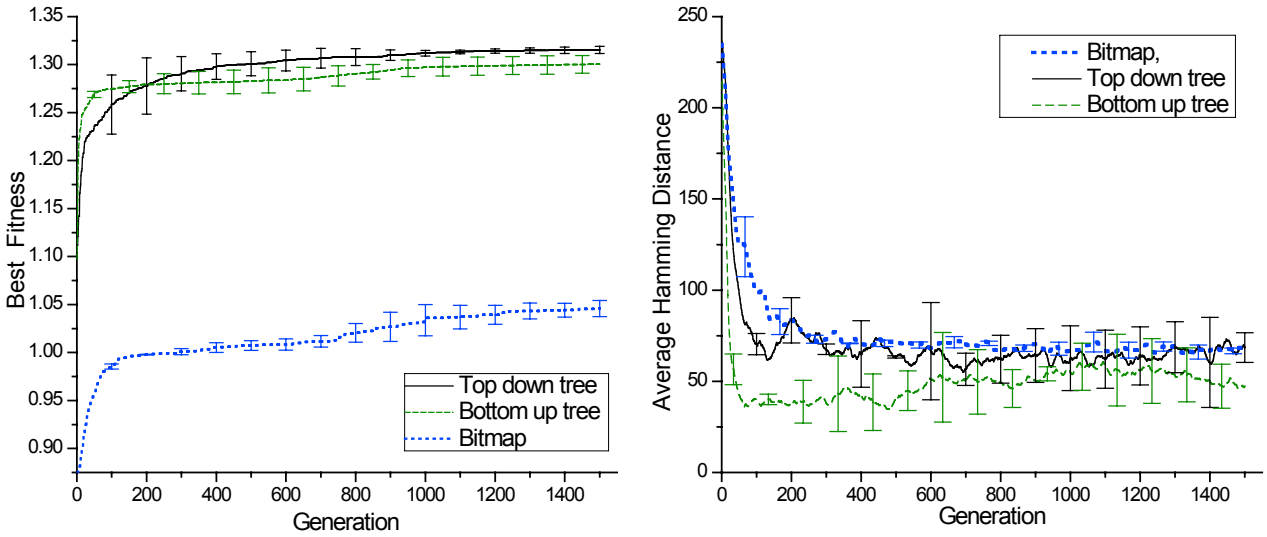


Fig. 8: Search performance of the SUS evolutionary algorithm. (a) Best fitness as a function of generation for each of the chromosome representations, (b) Average hamming distance as a function of generation. The curves were smoothed for presentation purposes. Error bars are derived from three independent runs started from randomized initial populations.

Figure 9 shows the results of the deterministic crowding evolutionary algorithm for the different types of chromosome representations. Using the bottom-up tree and top-down tree representations, the evolutionary algorithm yielded photonic crystals with bandgaps as large as 29.7% and 30.73%, respectively, comparable to the bandgaps achieved using stochastic-uniform-sampling. However, now the bitmap representation is able to achieve a bandgap as large as 21.32% on a 32x32 grid. The performance metrics are shown in Figure 10. The results are also compared with a completely random search (i.e. step 1 and 2 are repeated). The bitmap approach was also compared with a parallel hill climbing algorithm (i.e. the unit cells are randomly mutated, if there was an improvement the photonic crystal is kept, otherwise discarded). As seen in Figure 10a, the deterministic crowding evolutionary algorithm outperforms a completely random search for all of the representation types, consequently stochastic-uniform-sampling does too (See Figure 8). The evolutionary algorithms using the bitmap representation also outperform the parallel hill climbing algorithm, which only reaches a maximum bandgap of 1.71%. Figure 10b confirms that the deterministic crowding evolutionary algorithm is able to maintain a high-degree of diversity throughout all of the generations, enabling the vast improvement in the bitmap representations performance. However, when using the tree representations, deterministic crowding didn't offer a performance advantage over stochastic-uniform-sampling, even after 1500 generations.

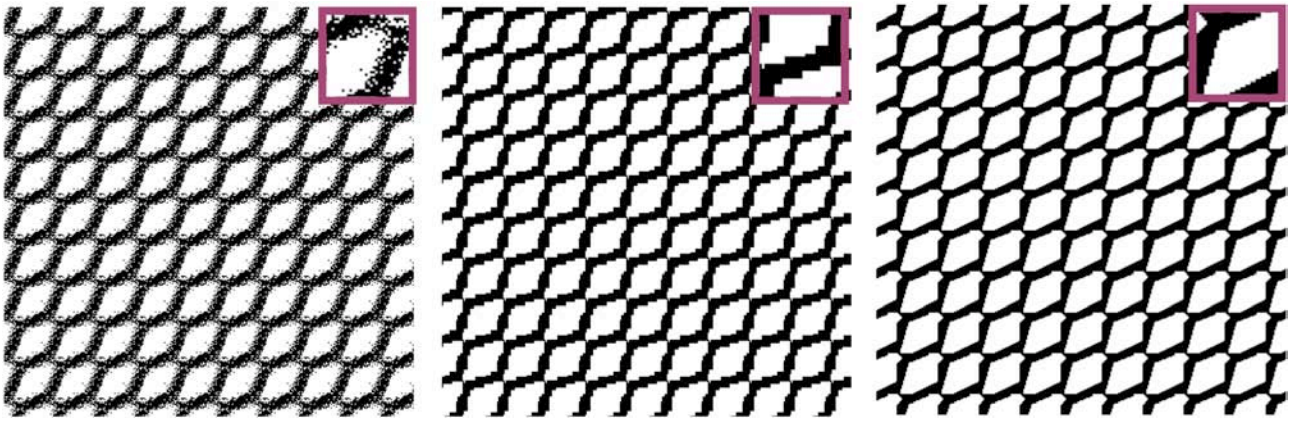


Fig. 9. Photonic crystals and unit-cells (insets) created by the deterministic crowding evolutionary algorithm. From left to right: Bitmap Representation (21.32% Bandgap), Bottom up tree (29.7% Bandgap), Top down tree (30.73% Bandgap)

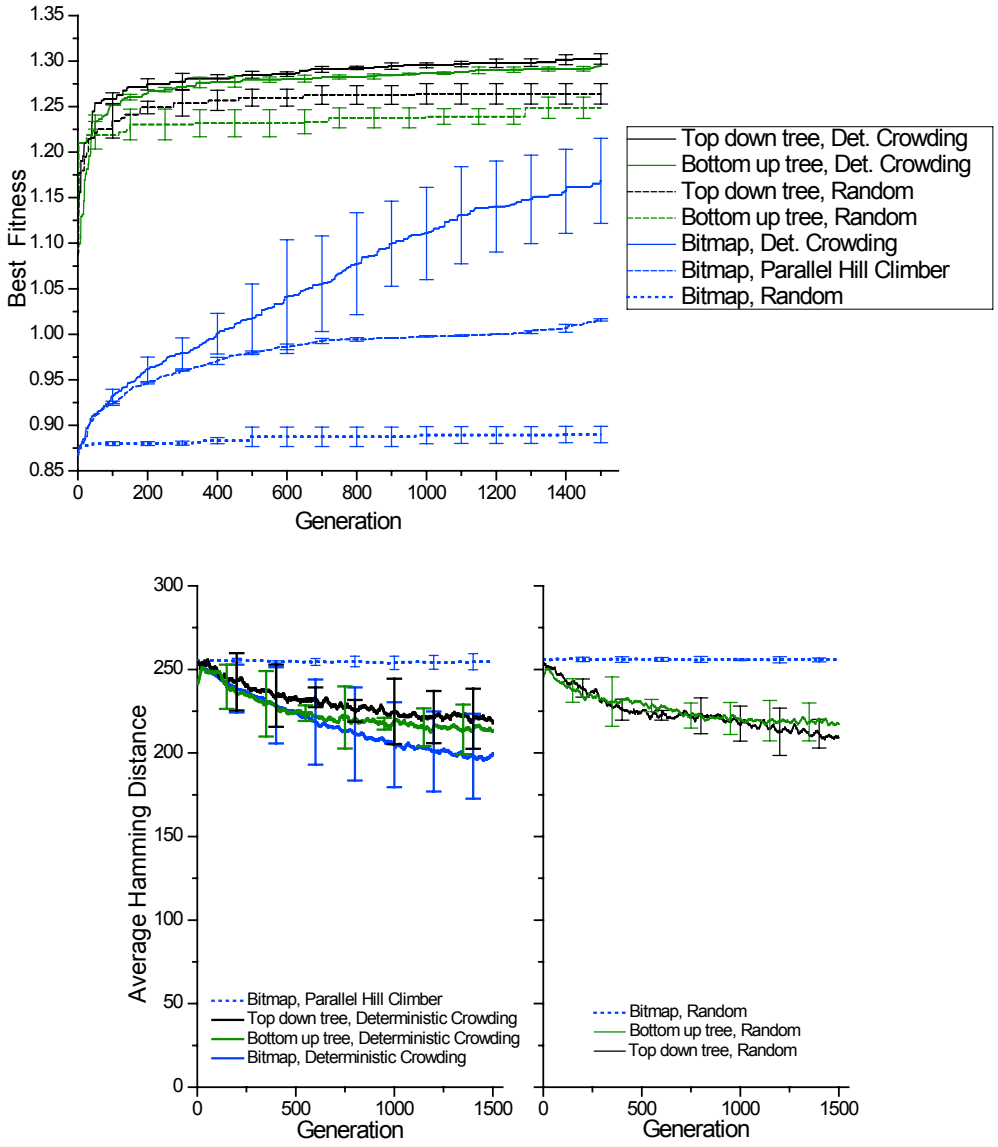


Fig. 10. Performance metrics for the deterministic crowding algorithm with the different chromosome representations. Comparisons to a random search algorithm and parallel hill climbing algorithm (only for the bitmap approach) are shown. a) Best fitness as a function of generation. The ordering in the legend corresponds with the ordering of the fitnesses on the graph (from best to worst). b) Average hamming distance as a function of generation. The curves were smoothed for presentation purposes. The left graph includes deterministic crowding and parallel hill climber. The right includes only random searches. Error bars are derived from three independent runs started from randomized initial populations.

As seen in Figure 10a, the random search (i.e. step 1 and 2 are repeated) achieved a best bandgap of 27.16% when using the top down tree representation. This is much better performance than all of the results obtained when using the bitmap representation. The reason for this is because of the tree representations efficient encoding of the unit cell. Despite the size of the grid, trees enable for an open-ended design space – i.e. the number of grid points can quadruple yet the tree is still able to encode the entire unit-cell without changing. The bitmap representation is plagued by 'rogue' pixels that reduce the effective index of the unit-cell, and this problem gets worse the finer the grid gets. Thus, the bitmap representation is best used with very coarse grids. Despite the very good performance of the random search, it is clear that an evolutionary algorithm was still needed to discover photonic crystals with even larger bandgaps.

We observed that the cross-over from a fitness below 1 to above 1 is very predictable (i.e. the population has no bandgaps and then develops bandgaps). A photonic crystal that may have a fitness of 0.98 in a previous generation (i.e. little to no overlap of the bands), after being crossed over and mutated with another parent *will* develop a small bandgap (~ 1%) in the next generation (of course, it's possible that after crossover and mutation that its fitness will decrease but *eventually* the right mating will occur), and consequently after many such generations develop into a photonic crystal with a rather large bandgap. This progression is predictable because as the photonic crystal bands develop less and less band overlap, structures evolve in the unit-cell that are able to support a bandgap. The bandgap arises once the structure is fine-tuned and the overall index-contrast is increased and subsequently the noise level is reduced. Even though the bitmap representation yielded a small bandgap when using a 32x32 grid and stochastic-uniform-sampling, the structure of a photonic crystal that *could* yield a large bandgap is very clearly seen in the noise of Figure 5. The evolutionary algorithm in fact found the correct structure; it was just unable to properly deal with the large amount of noise. This predictability shows that our overlap area fitness criteria is excellent for obtaining photonic crystals with large bandgaps when starting from 'random noise'.

The best published[15] human design for a photonic crystal using a square lattice and the TE polarization is shown in Figure 11. It has a bandgap of 28.35% for this index contrast (3.4 to 1). Our evolutionary algorithm has found photonic crystals that improve over this design by 12.5%. The evolutionary algorithm achieved this by not optimizing the human-designed structure but by finding new types of photonic crystal structures altogether. As seen in Figure 5 and 9, the photonic crystals discovered are highly-skewed and non-uniformly scaled. It has previously been shown that the bandgap of simple photonic crystals can sometimes be improved by reducing the symmetry of the unit cell and the lattice[15-17]. By making no assumptions about the symmetry of the unit cell, our evolutionary algorithm has found that the photonic crystals with the largest bandgaps tend to share this characteristic. This result has also been observed in nature, the photonic crystals in butterfly wings also exhibit a lack of strong symmetry and non-uniform scaling[18].

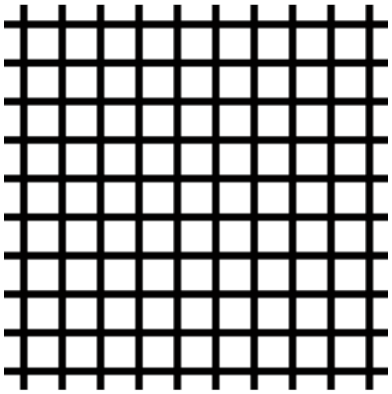


Fig. 11. Best human designed photonic crystal with a bandgap of 28.35%. The photonic crystal is a square lattice of square air (index -1) holes of width and height 0.8*a (a is the periodicity of the lattice) embedded in a background of high index material (index - 3.4).

4. CONCLUSIONS

We have demonstrated the ability to use evolutionary algorithms to discover novel photonic crystal structures with large bandgaps. Starting with a completely random population of photonic crystals that possess very small or even no bandgaps, we obtain photonic crystals with larger bandgaps than the best human design. We compared two types of selection criteria, stochastic-uniform-sampling and deterministic crowding, and two chromosome representations, bitmaps and trees. Each selection method and representation has advantages and disadvantages; so, future problems must be evaluated to determine the best approach for the problem. In practice, a combination of these techniques may yield the best results. For example, a bitmap representation would work very well for fine-tuning small regions of the unit-cells obtained from the tree representations. In conclusion, we've shown that evolutionary algorithms can be used as a robust design and optimization tool in the field of photonics.

ACKNOWLEDGEMENTS

The authors acknowledge support by the Cornell Center for Nanoscale Systems, supported by the National Science Foundation (NSF) and by the STC Program of the NSF. This work was performed in part at the Cornell Theory Center which is supported by its users, Cornell University and Industrial Affiliates.

REFERENCES

1. Biro L. P. et al., "Role of photonic-crystal-type structures in the thermal regulation of a Lycaenid butterfly sister species pair", Phys. Rev. E **67**, 021907 (2003).
2. Parker A. R., McPhedran R. C., McKenzie D. R., Botten L. C., Nicorovici N. A., "Photonic engineering: Aphrodite's iridescence", Nature **409**, 36-37 (2001).
3. Yablonovitch, E., "Inhibited spontaneous emission in solid-state physics and electronics", Phys. Rev. Lett. **58**, 2059 (1987).
4. Johnson S. G., Joannopoulos J. D., *Photonic Crystals: The Road from Theory to Practice,* (Kluwer, Boston, MA, 2002).
5. Joannopoulos J. D., Mead R. D., Winn J. N., *Photonic Crystals,* (Princeton University Press, Princeton, NJ, 1995).
6. Yablonovitch, E. et al., "Donar and acceptor modes in photonic band structure", Phys. Rev. Lett. **67**, 3380 (1991).
7. Yablonobitch, E., "Photonic band-gap structures", J. Opt. Soc. Am. B **10**, 283 (1993).
8. Holland J. H., *Adaptation in Natural and Artificial Systems*, (University of Michigan, Ann Arbor, 1975).
9. Mitchell M., *An introduction to genetic algorithms*, (MIT Press, 1996).
10. Koza J. R., Keane M. A., Streeter M. J., Mydlowec W., Yu J., and Lanza *G., Genetic Programming IV. Routine Human-Competitive Machine Intelligence*, (Kluwer, Boston, MA, 2003).
11. Lipson, H., Pollack J. B., "Automatic Design and Manufacture of Artificial Lifeforms", Nature **406**, pp. 974-978 (2000).
12. Shen L., Ye A., He S. , "Design of two-dimensional photonic crystals with large absolute band gaps using a genetic algorithm", Phys. Rev. B **68**, 035109 (2003).
13. Johnson S. G., Joannopoulos J. D., "Block-iterative frequency-domain methods for Maxwell's equations in a planewave basis", Optics Express **8**, 173-190 (2001).
14. Mahfoud S.W., *Niching methods for Genetic Algorithms*, Ph.D. dissertation from the University of Illinois, Urbana Champaign, IL, USA, (1995).
15. Susa N., "Large absolute and polarization-independent photonic band gaps for various lattice structures and rod shapes", J. Appl. Phys. **91**, 3501 (2002).
16. Anderson c. m., Giapis K.P., "Larger Two-Dimensional Photonic Band Gaps", Phys. Rev. Lett. **77**, 2949 (1996).
17. Qui M, He S., "Large complete band gap in two-dimensional photonic crystals with elliptic air holes", Phys. Rev. B **60**, 10610 (1999).
18. Poladian L., Large M., and Padden W., "Is the photonic crystal in the butterflies T. imperialis and P. sesostris optimal?", *CLEO 2004 Proceedings*.
19. Lipson H. (2004) "How to Draw a Straight Line Using a GP: Benchmarking Evolutionary Design Against 19th Century Kinematic Synthesis", Proceedings of Genetic and Evolutionary Computation Conference, Late Breaking Paper, GECCO 2004.